Decorrelated Neuronal Firing in Cortical Microcircuits

Alexander S. Ecker, *et al.*

Science **327**, 584 (2010);
DOI: 10.1126/science.1179867

Decorrelated Neuronal Firing in Cortical Microcircuits

Alexander S. Ecker,[1,2,3] Philipp Berens,[1,2,3] Georgios A. Keliris,[1] Matthias Bethge,[1,2] Nikos K. Logothetis,[1,4] Andreas S. Tolias[3,5,6]*

Correlated trial-to-trial variability in the activity of cortical neurons is thought to reflect the functional connectivity of the circuit. Many cortical areas are organized into functional columns, in which neurons are believed to be densely connected and to share common input. Numerous studies report a high degree of correlated variability between nearby cells. We developed chronically implanted multitetrode arrays offering unprecedented recording quality to reexamine this question in the primary visual cortex of awake macaques. We found that even nearby neurons with similar orientation tuning show virtually no correlated variability. Our findings suggest a refinement of current models of cortical microcircuit architecture and function: Either adjacent neurons share only a few percent of their inputs or, alternatively, their activity is actively decorrelated.

Correlated response fluctuations among simultaneously recorded neurons have been observed in a number of cortical areas (*1*–*14*). The prevailing hypothesis is that these correlations (referred to as "noise correlations") are caused by random fluctuations in the activity of neurons presynaptic to a pair of cells (*5*, *6*, *15*–*17*). Noise correlations are reported to be particularly strong in nearby cells with similar response properties (*5*–*13*, *18*), which supports the idea that nearby cells within a functional column are densely connected and share a substantial amount of common input (*17*). Theoretical work shows that noise correlations with such a "limited-range" structure are particularly detrimental for population coding (*5*, *19*–*21*). Thus, knowledge of the precise nature of noise correlations can advance our understanding of the structure and function of cortical microcircuits in vivo.

Although the prevalent finding of spike count correlations in the range of 0.1 to 0.3 (*2*–*11*) seems to suggest that their magnitude and cause have been firmly established, there are several technical challenges in the measurement of noise correlations. Spike count correlations can be generated in the absence of shared presynaptic noise by a number of factors: First, it is difficult to control for internal variables, which modulate firing rates, such as motor plans, or cognitive states, like attention. Second, recordings from electrodes that are not chronically implanted often suffer from instabilities in the electrodes' positions. Third, if multiple cells are recorded from the same electrode, suboptimal single-unit isolation is a concern (*22*). Fourth, in experiments conducted under anesthesia, correlations may arise from spontaneous oscillations that are absent in behaving animals (*23*). Given that all these factors will artificially increase estimates of noise correlations, it is important to control for every single one.

We reexamined this issue and measured spike count correlations by using arrays of chronically implanted tetrodes (fig. S1) to simultaneously record the activity of local groups of neurons in the primary visual cortex (area V1) of awake monkeys (*24*, *25*). Tetrodes provide a superior quality of single-unit isolation of nearby neurons (*26*) compared with conventional single electrodes or rigid multielectrode arrays. An example of a tetrode isolating multiple cells is shown in Fig. 1. Because the signal is recorded simultaneously by four adjacent microwires, the location of the neurons can be triangulated, resulting in distinct clusters, each representing the action potentials of a single neuron (Fig. 1, A and B). If, for example, only channel 4 had been recorded (as could be the case with a single electrode), cells 1, 2, 4, and 5 would have been nearly impossible to distinguish. For our analyses, we only considered cells that were quantitatively determined to be very well isolated, in this case discarding the second neuron, which had ~8% falsely assigned spikes (*25*). Cells recorded on one tetrode had highly overlapping receptive fields (Fig. 1C, colored outlines). We presented sine wave gratings drifting in 16 directions of motion perpendicular to the grating orientation (Fig. 1C). Consistent with the columnar organization of V1, three of the four neurons had very similar preferred orientations (Fig. 1D). When we examined the spike count correlations (r_{sc}) of the six pairs, they were extremely low (Fig. 1E), with an r_{sc} average value of 0.02.

We collected data in a total of 46 recording sessions from two monkeys (D, 27; H, 19). Gratings were presented at eight different orientations and were either static or drifting in the direction orthogonal to the orientation. The gratings were large enough to cover the receptive fields of all neurons recorded by the array (Fig. 1C). Spatial frequency and speed were chosen such that a large number of neurons was driven,

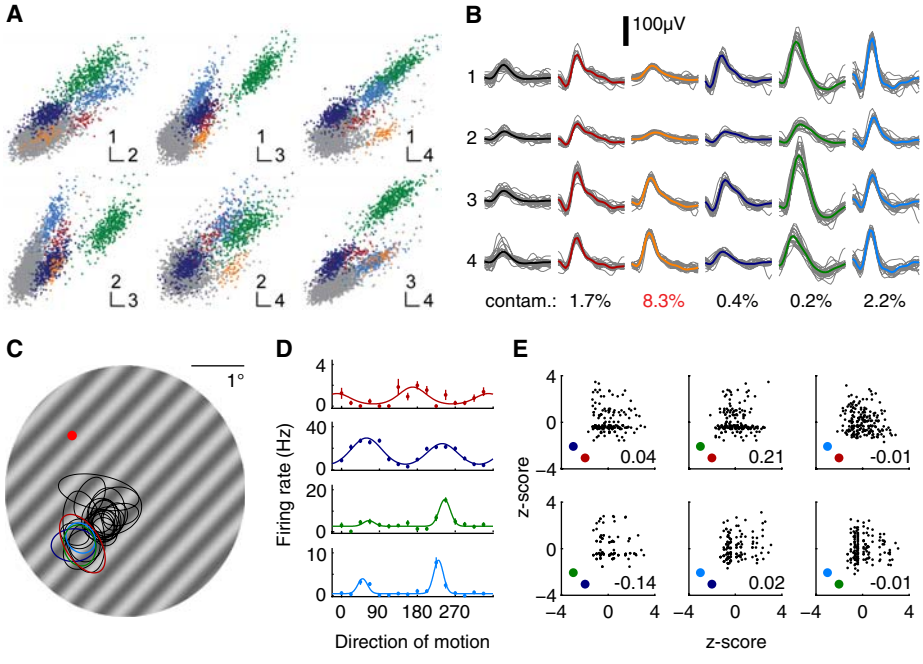

Fig. 1. Example of five single units recorded from one tetrode. Colors are matched in all panels. (**A**) Scatter plots showing amplitude of first principal component of spike waveforms for all pairs of channels. Clusters are modeled as multivariate Gaussians, which allows quantification of their separation. (**B**) Example waveforms of multiunit (black) and the five single units (colored). Each row corresponds to one tetrode channel. Estimated false-assignment rates (*25*) are shown below each column. Neuron 2 (orange) is discarded because of insufficient isolation. (**C**) Grating stimulus overlaid with receptive field outlines of 24 simultaneously recorded neurons. Red dot, fixation spot. (**D**) Tuning curves. Error bars are SEM. (**E**) Scatter plots of *z* score–transformed responses for all pairs obtained from the four neurons. r_{sc} values are indicated. Pair identities are coded by colored dots.

[1]Max Planck Institute for Biological Cybernetics, 72076 Tübingen, Germany. [2]Centre for Integrative Neuroscience and Institute for Theoretical Physics, University of Tübingen, 72076 Tübingen, Germany. [3]Department of Neuroscience, Baylor College of Medicine, Houston, TX 77030, USA. [4]Division of Imaging Science and Biomedical Engineering, University of Manchester, Manchester M1 7HL, UK. [5]Michael E. DeBakey Veterans Affairs Medical Center, Houston, TX 77030, USA. [6]Department of Computational and Applied Mathematics, Rice University, Houston, TX 77005, USA.

*To whom correspondence should be addressed: atolias@cns.bcm.edu

but not optimized for any specific cell. In total, we recorded 917 single units. After discarding cells that were not well isolated (>5% falsely assigned spikes), not visually responsive, or not tuned to orientation, we obtained 407 (D, 262; H, 145) single units. This corresponds to 1907 (D, 1335; H, 572) simultaneously recorded pairs, in 406 of which (D, 361; H, 45) both neurons were recorded by the same tetrode.

Neurons recorded from one tetrode are physically close to each other, have highly overlapping receptive fields, and are believed to receive strong common input. Nevertheless, spike count correlations in pairs of neurons recorded by the same tetrode were exceedingly low (r_{sc} = 0.005 ± 0.004; mean ± SEM) (Fig. 2). Even cells with similar preferred orientations (r_{signal} > 0.5) had very weak correlations (r_{sc} = 0.028 ± 0.010). This also held if pairs were strongly driven by gratings with orientations close to the cells' preferred orientations. Under such stimulation, spike count correlations were not larger than those under stimulation with less optimal gratings (r_{sc} = 0.021 ± 0.013 versus 0.016 ± 0.011, two-sample *t* test: *P* = 0.80, *n* = 361). Only ~14% of all pairs with cells recorded from the same tetrode had correlations significantly different from zero (α = 0.05; for r_{signal} > 0.5: 13.2% positive, 2.4% negative; for r_{signal} < 0.5: 5.9% positive, 7.4% negative). Theoretical considerations and numerical studies indicate that much of the scatter in the distribution (Fig. 2B) may result from estimating correlation coefficients from finite data (figs. S2 and S3). Even though there were cases where similarly tuned neurons were correlated, these constituted only a small minority of pairs. Under our experimental conditions, spike count correlations for local ensembles were smaller than previously reported by more than an order of magnitude (Fig. 2C).

Previous studies report high correlations also for similarly tuned cells recorded on different electrodes separated by up to several millimeters (*7*–*11*). Therefore, we analyzed all simultaneously recorded pairs, including those pairs where the two neurons were recorded by different tetrodes. Average spike count correlations were low (r_{sc} = 0.010 ± 0.002, mean ± SEM) (Fig. 3, A and B). There was only a weak relation between tuning similarity and spike count correlation (two-sample *t* test, r_{signal} < 0.5 versus r_{signal} > 0.5: *P* = 0.003, *n* = 1907) (Fig. 3C), and even similarly tuned cells had an average correlation close to zero (r_{signal} > 0.5: r_{sc} = 0.023 ± 0.005, mean ± SEM) (Fig. 3C). Correlations did not depend on the distance between the two neurons (linear regression slope: *P* = 0.99; two-sample *t* test within versus across tetrodes: *P* = 0.16) (Fig. 3D). Although there was a weak relation between two neurons' average firing rate and their spike count

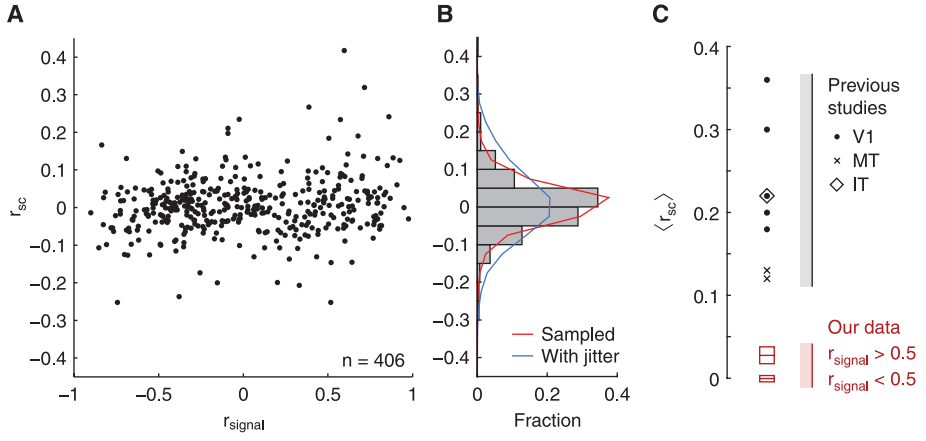

Fig. 2. Spike count correlations of pairs of neurons recorded by the same tetrode. (**A**) Relation between r_{signal} and r_{sc} for all pairs of nearby neurons (both neurons recorded by the same tetrode). (**B**) Distribution of r_{sc} (mean ± SEM = 0.005 ± 0.004). Colored lines are distributions obtained by generating artificial data with the same number of trials as in the experiments (red, fixed r_{sc} = 0.01; blue, average r_{sc} = 0.01 and S.D. 0.1), which indicate that most of the scatter in the empirical distribution is due to estimating correlations from finite data [see supporting online material (SOM) text sections 1 and 2 for discussion]. (**C**) Average r_{sc} compared with previously reported values [black symbols, V1 (*3*, *4*, *7*–*9*); MT (*5*, *6*); IT (*2*)]. Cells with similar tuning (r_{signal} of >0.5) have slightly higher correlations (r_{sc} = 0.028 ± 0.010) than dissimilar cells (r_{sc} = –0.001 ± 0.004, two-sample *t* test, *P* = 0.002, *n* = 406), but r_{sc} is an order of magnitude smaller than in previous reports.

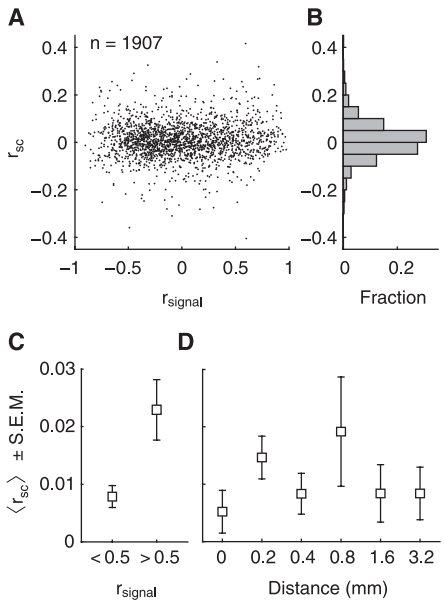

Fig. 3. (**A**) Relation between r_{signal} and r_{sc} for all pairs of simultaneously recorded neurons. (**B**) Distribution of r_{sc} (mean ± SEM = 0.010 ± 0.002). (**C**) Cells with similar tuning (r_{signal} of >0.5) have slightly higher correlations (r_{sc} = 0.023 ± 0.005) than the remaining cells (r_{sc} = 0.008 ± 0.002, two-sample *t* test, *P* = 0.025, *n* = 1907). (**D**) r_{sc} values do not depend on the distance between neurons (linear regression: *P* = 0.99, *n* = 1907). The bin at zero contains neurons recorded by the same tetrode (Fig. 2). Error bars show SEM.

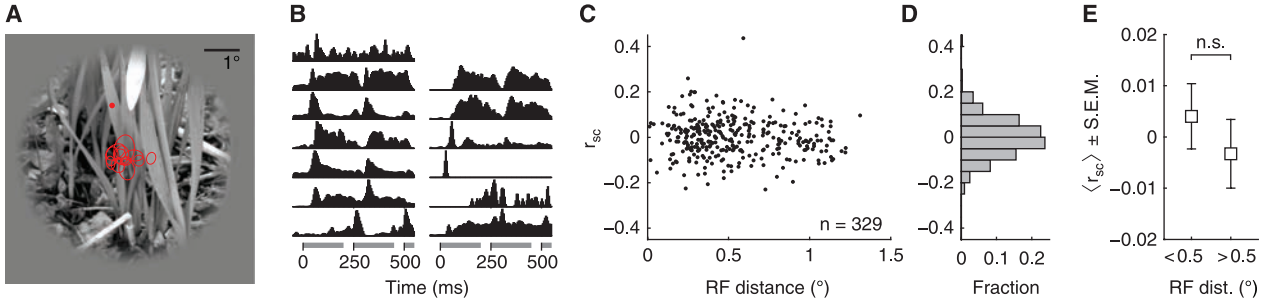

Fig. 4. Spike count correlations for natural images. (**A**) Example of the stimulus with receptive field outlines of 13 simultaneously recorded neurons. Red dot, fixation spot. (**B**) Peristimulus time histograms of cells in (A) for this stimulus. In each trial, the stimulus was flashed four times for 200 ms, with 50-ms pauses. For consistency with the grating stimulus, spike counts were computed from the first 500 ms (two stimulus flashes). (**C**) Relation between receptive field distance and r_{sc} is not significant (linear regression: *P* = 0.11, *n* = 329). (**D**) Distribution of r_{sc} (mean ± SEM = 0.001 ± 0.005). (**E**) Average r_{sc} for pairs with overlapping receptive fields versus pairs with nonoverlapping receptive fields. Two-sample *t* test: *P* = 0.89, *n* = 329.

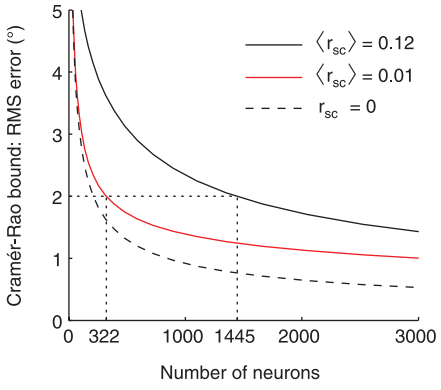

Fig. 5. Impact of correlation strength on encoding accuracy of neural populations. The Cramér-Rao bound (minimum achievable decoding error) is shown for different correlation structures: a previous report [black, refs. (*5*, *6*)], our data (red), and an independent population of neurons (black dashed). Dotted lines highlight the number of neurons that would be necessary to achieve a decoding error of 2°. For details, see fig. S8 and SOM text, section 6.

correlations, this relation arose on time scales longer than one trial and therefore appears to be unrelated to shared presynaptic noise (fig. S4).

To investigate whether low correlations also occur under more naturalistic stimulus conditions, we conducted additional experiments in one of the monkeys (H). We first mapped the neurons' receptive fields before presenting natural images (Fig. 4, A and B) (*25*). The average r_{sc} was close to zero (r_{sc} = 0.001 ± 0.005, mean ± SEM, one-sample *t* test: P = 0.89, n = 329) (Fig. 4, C and D), with no relation between receptive field overlap and spike count correlations (linear regression slope: P = 0.12, n = 329) (Fig. 4C). Neurons with receptive fields within 0.5° of visual angle had spike count correlations similar to neurons with more distant receptive fields (two-sample *t* test: P = 0.43, n = 329) (Fig. 4E).

We recorded another 56 pairs of neurons while a third monkey (B) was presented with moving bars. As with the other stimuli, spike count correlations were close to zero under these conditions (0.014 ± 0.011, mean ± S.E.M, P = 0.21, n = 56) (fig. S5).

Under a variety of stimulation conditions ranging from classic stimuli (such as bars and gratings) to natural images, spike count correlations in the primary visual cortex of awake monkeys were extremely low. These results stand in contrast to a number of previous studies, which report correlations of the order 0.1 to 0.3. Above we suggested four factors that could lead to spike count correlations unrelated to shared presynaptic noise (*27*). We now demonstrate how artificially introducing any one of these into our data produces correlations similar to previously published results. First, uncontrolled external or internal variables can be studied by assuming the neurons' firing rates are gain-modulated by a common underlying process. Shared modulations of only ~15% can lead to correlations on the order of 0.2, as shown in fig. S6. It is extremely hard, if not impossible, to control precisely the effects of attentional state, reward expectancy, task-solving strategy, or other cognitive factors (*28*). In contrast to extrastriate areas like V4 or MT, area V1 is much less affected by such modulations. Second, slow drifts over time or abrupt movements of the electrode tip can lead to changing waveforms and, thus, lost spikes or increased contamination by multiunit activity because of decreasing signal-to-noise ratio. Because movement is likely to affect all neurons recorded by one electrode, it can be modeled as a common gain modulation, and the above arguments apply. Our recordings were extraordinarily stable, as demonstrated by our ability to track neurons over several days (*24*). Third, contamination of waveform clusters identified as single units by spikes of other cells can create artificially high correlations and can even give rise to or amplify the limited-range correlation structure (fig. S7 shows that ~10% false assignments during spike sorting can produce correlations of order 0.1). Fourth, during anesthesia, up and down states or even subtle variations in the level of anesthesia will inevitably cause changes in firing rates common to many cells [analogous to point 1 but on a relatively rapid time scale; see also (*29*)], potentially having a stronger impact on nearby cells. Thus, any meaningful characterization of the impact of noise correlations on population coding critically depends on the ability to obtain stable recordings from large populations of well-isolated adjacent neurons, ideally in an awake animal and in a cortical region like V1, which is not modulated strongly by variables that cannot be precisely controlled. Interpreting spike count correlations in terms of their effects on encoding capacities of cortical microcircuits or drawing conclusions about functional connectivity only makes sense if one can separate covariability because of uncontrolled variables from that reflecting intrinsic noise in the circuit.

Our findings have implications for models of cortical circuit architecture. The current view on the generation of correlations in cortical circuits rests on two major assumptions: (i) nearby cortical neurons receive a substantial amount of common input (*6*, *17*, *30*, *31*); (ii) such common input leads to correlations (*15*–*17*, *32*). In light of our data, at least one of these assumptions cannot be correct.

Based on measured spike count correlations, an influential modeling study inferred that, on average, nearby cells share up to 30% of their inputs (*17*). Under the same model, our data suggest that at most, 5% of the inputs are shared. Note that anatomical studies report ~10% common inputs for excitatory neurons (*30*, *31*). In addition, cortical excitatory connections may be very precisely structured (*33*) to form many independent subunits. In this case, most recorded pairs consist of neurons belonging to different subunits, and average correlations are very low.

Assumption (ii) has been challenged by recent network models in which a dynamic balance of excitatory and inhibitory fluctuations counteracts correlations induced by common inputs (*29*, *34*). This results in correlations that are positive on average but very low (~0.01), a prediction in good agreement with our data. To prevent small correlations from accumulating and dominating network activity, such a decorrelation mechanism might be a crucial prerequisite of hierarchical cortical processing.

Whatever the mechanism behind the decorrelated state of the neocortex, it offers substantial advantages for information processing: Consider a downstream neuron reading out the orientation of a grating from the activity of V1 neurons. If correlations were ~0.12 on average (*5*, *6*), the number of neurons necessary to achieve 2° precision (root mean square error) would be five times larger than those in the scenario in which the average correlations are ~0.01 (Fig. 5 and fig. S8). Moreover, it is unclear whether neurons have access to the correlation structure of their synaptic inputs. If the network is in the decorrelated state, however, the effect of not taking any remaining correlations into account is small, and decoding is greatly simplified.

References and Notes

1. M. Bach, J. Krüger, *Exp. Brain Res.* **61**, 451 (1986).
2. T. J. Gawne, B. J. Richmond, *J. Neurosci.* **13**, 2758 (1993).
3. T. J. Gawne, T. W. Kjaer, J. A. Hertz, B. J. Richmond, *Cereb. Cortex* **6**, 482 (1996).
4. D. S. Reich, F. Mechler, J. D. Victor, *Science* **294**, 2566 (2001).
5. E. Zohary, M. N. Shadlen, W. T. Newsome, *Nature* **370**, 140 (1994).
6. W. Bair, E. Zohary, W. T. Newsome, *J. Neurosci.* **21**, 1676 (2001).
7. A. Kohn, M. A. Smith, *J. Neurosci.* **25**, 3661 (2005).
8. D. A. Gutnisky, V. Dragoi, *Nature* **452**, 220 (2008).
9. M. A. Smith, A. Kohn, *J. Neurosci.* **28**, 12591 (2008).
10. M. R. Cohen, W. T. Newsome, *Neuron* **60**, 162 (2008).
11. X. Huang, S. G. Lisberger, *J. Neurophysiol.* **101**, 3012 (2009).
12. D. Lee, N. L. Port, W. Kruse, A. P. Georgopoulos, *J. Neurosci.* **18**, 1161 (1998).
13. C. Constantinidis, P. S. Goldman-Rakic, *J. Neurophysiol.* **88**, 3487 (2002).
14. B. B. Averbeck, D. Lee, *J. Neurosci.* **23**, 7630 (2003).
15. H. L. Bryant Jr., A. R. Marcos, J. P. Segundo, *J. Neurophysiol.* **36**, 205 (1973).
16. A. M. Aertsen, G. L. Gerstein, M. K. Habib, G. Palm, *J. Neurophysiol.* **61**, 900 (1989).
17. M. N. Shadlen, W. T. Newsome, *J. Neurosci.* **18**, 3870 (1998).
18. B. B. Averbeck, D. Lee, *J. Neurophysiol.* **95**, 3633 (2006).
19. L. F. Abbott, P. Dayan, *Neural Comput.* **11**, 91 (1999).
20. S. D. Wilke, C. W. Eurich, *Neural Comput.* **14**, 155 (2002).
21. H. Sompolinsky, H. Yoon, K. Kang, M. Shamir, *Phys. Rev. E Stat. Nonlin. Soft Matter Phys.* **64**, 051904 (2001).
22. K. D. Harris, D. A. Henze, J. Csicsvari, H. Hirase, G. Buzsáki, *J. Neurophysiol.* **84**, 401 (2000).
23. J. F. Poulet, C. C. Petersen, *Nature* **454**, 881 (2008).
24. A. S. Tolias *et al.*, *J. Neurophysiol.* **98**, 3780 (2007).
25. Materials and methods are available as supporting material on *Science* Online.
26. C. M. Gray, P. E. Maldonado, M. Wilson, B. McNaughton, *J. Neurosci. Methods* **63**, 43 (1995).
27. Although many studies were in V1 (*1*, *3*, *4*, *7*–*9*), for some studies, area differences could play a role (*2*, *5*, *6*, *10*–*13*). In addition, different recording methods might be biased toward recording certain types of cells. However, tetrodes have also been used before (*4*).
28. In addition, miniature eye movements are known to modulate firing rates, a problem that is amplified if

small stimuli, barely covering the neurons' receptive fields, are used.
29. A. Renart *et al.*, *Science* **327**, 587 (2010).
30. V. Braitenberg, A. Schüz, *Anatomy of the Cortex: Statistics and Geometry* (Springer, Berlin, 1991).
31. B. Hellwig, A. Schüz, A. Aertsen, *Biol. Cybern.* **71**, 1 (1994).
32. J. de la Rocha, B. Doiron, E. Shea-Brown, K. Josić, A. Reyes, *Nature* **448**, 802 (2007).
33. Y. C. Yu, R. S. Bultje, X. Wang, S. H. Shi, *Nature* **458**, 501 (2009).
34. J. Hertz, *Neural Comput.*, published online 20 October 2009; 10.1162/neco.2009.06-08-806.

35. We thank M. Subramanian, A. Hoenselaar, T. J. Williford, and D. Murray for help with experiments; R. J. Cotton for his contribution in setting up recording equipment; and the Siapas laboratory at Caltech for providing the recording software. We thank R. J. Cotton, P. Dayan, S. Deneve, K. D. Harris, E. V. Lubenov, W. J. Ma, J. H. Macke, A. Renart, J. de la Rocha, A. G. Siapas, and S. M. Smirnakis for comments on the manuscript and discussions. This work was supported by the National Eye Institute, NIH (R01 EY018847), the Max Planck Society, the U.S. Department of Defense (W81XWH-08-2-0147), a VA Merit Award from the Department of Veterans Affairs, and an Arnold and Mabel Beckman Foundation Young Investigator Award to A.S.T., and by the German Federal Ministry of Education and Research (BMBF) through the Bernstein award to M.B. (FKZ:01GQ0601).

Supporting Online Material

www.sciencemag.org/cgi/content/full/327/5965/584/DC1
Materials and Methods
SOM Text
Figs. S1 to S9
References

29 July 2009; accepted 10 December 2009
10.1126/science.1179867

The Asynchronous State in Cortical Circuits

Alfonso Renart,[1]*‡ Jaime de la Rocha,[1,2]* Peter Bartho,[1,3] Liad Hollender,[1] Néstor Parga,[4] Alex Reyes,[2] Kenneth D. Harris[1,5]†

Correlated spiking is often observed in cortical circuits, but its functional role is controversial. It is believed that correlations are a consequence of shared inputs between nearby neurons and could severely constrain information decoding. Here we show theoretically that recurrent neural networks can generate an asynchronous state characterized by arbitrarily low mean spiking correlations despite substantial amounts of shared input. In this state, spontaneous fluctuations in the activity of excitatory and inhibitory populations accurately track each other, generating negative correlations in synaptic currents which cancel the effect of shared input. Near-zero mean correlations were seen experimentally in recordings from rodent neocortex in vivo. Our results suggest a reexamination of the sources underlying observed correlations and their functional consequences for information processing.

The spiking activity of neurons is often correlated within local cortical populations (*1*–*4*). Although correlations could be a signature of active information processing (*5*, *6*), they can also impair the estimation of information conveyed by the firing rates of neural populations (*7*, *2*, *8*) and might limit the efficiency of an organism for performing sensory discriminations (*7*, *2*). Under special conditions, correlated spiking is an inevitable consequence of shared presynaptic input (*9*, *10*). In general, however, the overall contribution of shared input to correlation magnitudes measured in vivo is unclear, as measured correlations could reflect mostly covariations in activity due to cognitive or external variables outside the control of the experimenter (*11*–*13*). To investigate the relation between correlations and shared input, we studied theoretically the correlation structures characteristic of densely connected recurrent networks.

We start by considering how the correlation between a single neuronal pair depends on the fraction p of shared inputs and the degree r_{in} to which the inputs are themselves correlated. The effect of shared input can be isolated by considering presynaptic neurons that fire independently ($r_{in} = 0$). Both excitatory (E) and inhibitory (I) shared inputs cause positive correlations of a moderate magnitude in the synaptic input and spiking activity of the postsynaptic pair (Fig. 1, A and B) (*9*, *14*). Spiking correlations r_{in} between inputs, however, have a major impact on the output correlation r_{out} of the postsynaptic pair. When all inputs are E, weak input correlations give rise to strongly correlated synaptic currents and output spikes (Fig. 1C). This occurs because, when p and r_{in} are small, the correlation c of the two input currents is approximately equal to

$$c \simeq p + Nr_{in} \qquad (1)$$

(*15*), where N is the number of synaptic inputs, resulting in a large gain in the relation between r_{in} and r_{out} (Fig. 1E, upper solid curve). The situation changes when both neurons receive I as well as E inputs. Correlations between E or between I neurons lead to strongly cor-

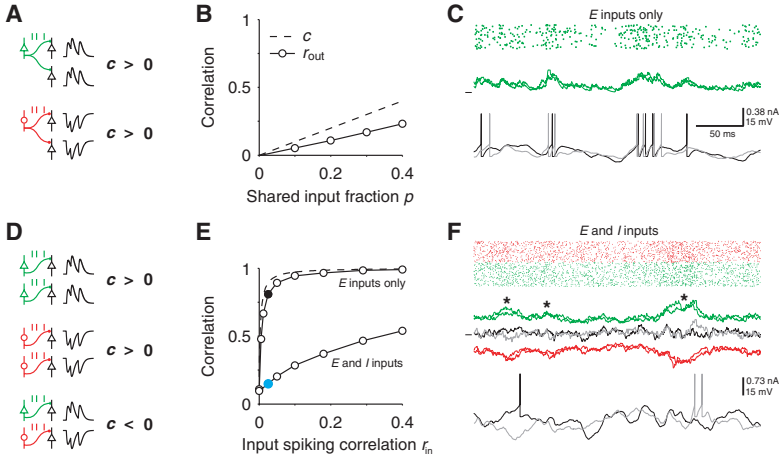

Fig. 1. Effect of shared inputs and correlated inputs on output correlation. (**A**) Shared excitatory (E, green) or inhibitory (I, red) inputs induce positive correlations in the synaptic currents of two cells ($c > 0$). (**B**) Correlation coefficient of synaptic currents c (dashed line) and output spikes r_{out} (circles, count window 50 ms) of a postsynaptic pair of integrate-and-fire neurons as a function of the shared input fraction p (*21*). Each postsynaptic cell received $N_E = 250$ Poisson input spike trains. (**C**) Input spike raster (top), synaptic currents (middle), and membrane potentials (bottom) of a postsynaptic pair receiving weakly correlated E inputs [black circle in (E), $r_{in} = 0.025$]. (**D**) Whereas correlations between E inputs or between I inputs contribute positively to c, correlations between E and I inputs have a decorrelating effect. (**E**) Correlations c (dashed line) and r_{out} (circles) as a function of the input spike correlation r_{in} at fixed $p = 0.2$. E inputs only: Each cell receives $N_E = 250$ correlated Poisson spike trains (*21*); E and I inputs: $N_I = 220$ inhibitory input trains were added with identical statistics and correlations. (**F**) Same as (C) but for the case with E and I inputs [blue circle in (E), $r_{in} = 0.025$]. E and I currents are shown separately from the total currents (black and gray). Asterisks indicate large fluctuations in the excitatory and inhibitory currents that occur simultaneously.

[1]Center for Molecular and Behavioral Neuroscience, Rutgers University, Newark, NJ 07102, USA. [2]Center for Neural Science, New York University, New York, NY 10003, USA. [3]Institute of Experimental Medicine, Hungarian Academy of Sciences, Budapest 1083, Hungary. [4]Departamento de Física Teórica, Universidad Autónoma de Madrid, Madrid 28049, Spain. [5]Smilow Research Center, New York University Medical School, New York, NY 10016, USA.

*These authors contributed equally to this work.
†Present address: Departments of Bioengineering and Electrical and Electronic Engineering, Imperial College, London SW7 2AZ, UK.
‡To whom correspondence should be addressed. E-mail: arenart@andromeda.rutgers.edu